Asymmetric electron bilayer: A molecular dynamics study of correlations and diffusion

S. Ranganathan
Department of Physics, Royal Military College of Canada, Kingston, Ontario, Canada K7K 7B4

R. E. Johnson
Department of Mathematics and Computer Science, Royal Military College of Canada, Kingston, Ontario, Canada K7K 7B4

(Received 21 August 2008; revised manuscript received 17 October 2008; published 24 November 2008)

Molecular dynamics simulations of a classical asymmetric electron bilayer for various values of the interlayer separation distance d and various degrees of asymmetry have been performed. The number of charged particles in the basic cell of one layer was fixed at 512, corresponding to a coupling strength $\Gamma(=\frac{e^2}{ak_BT})$ of 80, while that of the other varied from 32 to 512 particles, corresponding to a Γ of 20 to 80; a is the Wigner-Seitz radius. We have analyzed the intralayer and interlayer pair-correlation functions and the self-diffusion coefficients of the two layers and compared them with those of a symmetric electron bilayer. It is found that the self-diffusion coefficients of the two layers do not differ significantly for values of $d \leq 0.8$ with a marked deviation setting for $d=2$. A fluid-solid phase transition, observed previously for the symmetric bilayer for certain values of d, no longer exists even for the slightly asymmetric (512,450) bilayer we considered.

DOI: 10.1103/PhysRevB.78.195323 PACS number(s): 68.65.Ac, 52.65.Yy

I. INTRODUCTION

Strongly coupled charged-particle bilayers have been a subject of considerable research over the past decade and more. In such systems, each layer is made up of identical charged particles and immersed in a uniform neutralizing background of the opposite charge. For the most part, these studies have been confined to symmetric bilayers where the density of the charged particles is the same in the two layers. Static and dynamic properties of classical and symmetric bilayer systems made up of charges of the same sign have been investigated through molecular dynamics (MD) (Refs. 1–5) and theoretical models.[6–8] Symmetric electron-hole systems in which the two layers are made up of charged particles of opposite signs but have same density have also been investigated.[9–12] Properties of such systems depend only on two parameters: the interlayer separation d and the classical plasma coupling parameter $\Gamma=\frac{e^2}{ak_BT}$, the ratio of the average potential energy to the average kinetic energy per particle. $a=(n\pi)^{-1/2}$ is the Wigner-Seitz (WS) radius, with n as the areal density, k_B as the Boltzmann constant, e as the electronic charge, and T as the temperature. However asymmetric bilayers, in which the two layers have different charged-particle density, have not received much attention.[13,14] This asymmetry introduces another parameter: the ratio of the two densities or equivalently in the MD simulations, the number of charged particles in the basic cell in each of the two layers. Such systems are of importance, for example, in semiconductors. We have performed MD simulations to study how the self-diffusion coefficients of the two layers are affected by the asymmetry. The intralayer pair distribution functions (pdfs) $g_{11}(r)$ and $g_{22}(r)$ have also been obtained and analyzed.

II. SIMULATION DETAILS

The system to be simulated is a bilayer with different densities in the layers. We have used square basic cells of the same size in both layers and periodic boundary conditions. We take there to be N_1 electrons in the lower layer and N_2 electrons in the upper layer, all interacting through a $1/r$ Coulomb potential. Subscripts "1" and "2" on any quantity refer to the lower and upper layers, respectively. These layers are parallel planes separated by a distance d; each particle is constrained to move only in its original plane. Charge neutrality in each plane is guaranteed by embedding the particles in a uniform background of opposite charge. The thermodynamic state of the system is specified by Γ_1, Γ_2, and d. The temperature is kept the same in both the layers, but the coupling strength Γ is different since the WS radii for the two layers are different.

Details of the simulation and the extended Ewald sum technique have been described in our earlier paper.[15] For the sake of completeness, we include some of the essential features of our method here. The dynamics in our MD simulation needs the force, and, as an example, the force on any one particle in the lower plane due to all particles in both planes is given by

$$\begin{aligned}\vec{F}(\vec{r}_1) = \frac{2\pi}{L^2}\sum_{\vec{g}\neq\vec{0}}\vec{g}\Bigg\{&\frac{1}{g}\mathrm{erfc}\left(\frac{g}{2\alpha}\right)\sum_{j=2}^{N_1}\sin[\vec{g}\circ(\vec{r}_1-\vec{r}_j)] \\ &+\psi(g;\kappa,d)\sum_{j=1}^{N_2}\sin[\vec{g}\circ(\vec{r}_1-\vec{\rho}_j)]\Bigg\} \\ &+\sum_{\vec{p}}{}'\sum_{j=1}^{N_1}\frac{\vec{s}_{1j}}{|\vec{s}_{1j}|^3}\Bigg\{\mathrm{erfc}(\alpha|\vec{s}_{1j}|) \\ &+\alpha|\vec{s}_{1j}|\frac{2}{\sqrt{\pi}}\exp(-\alpha^2|\vec{s}_{1j}|^2)\Bigg\} \\ &+\sum_{\vec{p}}\sum_{j=1}^{N_2}\frac{\vec{d}_{1j}}{|\vec{d}_{1j}|^3}\Bigg\{\mathrm{erfc}(\kappa|\vec{d}_{1j}|) \\ &+\kappa|\vec{d}_{1j}|\frac{2}{\sqrt{\pi}}\exp(-\kappa^2|\vec{d}_{1j}|^2)\Bigg\}, \end{aligned} \quad (1)$$

where

$$\psi(g;\kappa,d) = \int_0^\infty dr \frac{r}{\sqrt{r^2+d^2}} \mathrm{erf}(\kappa\sqrt{r^2+d^2}) J_0(gr)$$
$$= \frac{1}{2g}\left[e^{gd}\,\mathrm{erfc}\left(\frac{g}{2\kappa}+\kappa d\right) + e^{-gd}\,\mathrm{erfc}\left(\frac{g}{2\kappa}-\kappa d\right)\right]. \quad (2)$$

The layers are separated by a distance d along the z axis; then $\vec{s}_{1j}=\vec{r}_1-\vec{r}_j+\vec{p}$ and $\vec{d}_{1j}=\vec{r}_1-\vec{\rho}_j+\vec{d}+\vec{p}$, where $\vec{r}_i$ denotes the position of the ith particle in the same (x,y) plane and $\vec{\rho}_j$ the position of the jth particle in the other (x,y) plane; L is the length of the square simulation cell. The sum over $\vec{p}$ is a sum over integers k_1 and k_2 with $\vec{p}=L(k_1,k_2)$; the prime on this sum implies that if $\vec{p}=\vec{0}$, the $i=j$ term is to be omitted. The sum over $\vec{g}$ is a sum over integers λ_1 and λ_2 with $\vec{g}=\frac{2\pi}{L}(\lambda_1,\lambda_2)$. The Ewald parameters α and κ are chosen so that both series in Eq. (1) converge rapidly; our analysis indicates that an optimum choice for both these parameters is $8/L$. Acceptable accuracy for the sum in the first term of Eq. (1) can be obtained using $|\vec{\lambda}|$ as small as 5; however we used $|\vec{\lambda}|<10$ in the calculations presented here. This is sufficiently large so that only the $\vec{p}=\vec{0}$ terms in the p summation in Eq. (1) need to be retained, implying that the real-space terms vanish at a distance corresponding to $L/2$. All quantities involved are in dimensionless units: distance in units of WS radius a_1, time in units of $\tau=\sqrt{\frac{ma_1^3}{e^2}}$, and energies in units of e^2/a_1. Even though the two layers do not have the same surface density, we have kept the basic cell in our MD simulation as a square with the same side length $L=(\frac{N_1}{n_1 a_1^2})^{1/2}=(\frac{N_2}{n_2 a_1^2})^{1/2}$ in both the layers. Using the definition of the WS radius, this then yields the relation between the coupling strengths in the two layers as

$$\Gamma_2 = \Gamma_1 \frac{a_1}{a_2} = \Gamma_1 \sqrt{\frac{N_2}{N_1}}. \quad (3)$$

We chose $N_1=512$ and $N_2=2k^2$ with k taking on integer values from 4 to 16, yielding the smallest value of Γ_2 as $\Gamma_1/4$. These values of N_1 and N_2 allow us to have a face-centered structure as our starting configuration in each of the layers. The dimensionless temperature T (in units of $1/k_B$) is then given by $1/\Gamma_1$ which was kept the same in both layers. The desired temperature was reached by scaling the velocities of the electrons in each of the two layers at regular time intervals. Once the equilibrium was achieved, the system was allowed to evolve without any temperature scaling. The temperatures of both layers were monitored, and they did not vary by more than 2%. Our MD simulation provides the position vector $\vec{r}_k(t)=[x_k(t),y_k(t)]$ and the velocity vector $\vec{v}_k(t)=[v_{kx}(t),v_{ky}(t)]$ for $k=1$ to N_1 (or N_2) particles in each of the two layers and for 10 000 times separated by a time step of 0.06. These data are then used to obtain the various correlation functions. Simulations were performed for one value of $\Gamma_1=80$ for several values of d from 0.1 to 4.0 and for 13 values of N_2 from 32 to 512. A bilayer is described by the number of particles in each of the lower and upper layers and will be denoted by $(512,N_2)$. We chose $\Gamma_1=80$ since for this value of the coupling constant, we have performed extensive MD simulations for a symmetric bilayer.[2,4] We could then readily compare the results of symmetric and asymmetric bilayers to see how the presence of a layer with different densities would affect the properties in a given layer. It has been shown, for example, that a symmetric bilayer with $\Gamma=80$ exhibits a phase transition at intermediate values of d,[2,5] and it would be very interesting to see whether or not an asymmetric bilayer shows such a behavior.

III. RESULTS

The MD data for the position vector and the velocity vector for any specific value of Γ and d can then be used to obtain the corresponding static or dynamic correlation function. The quantities of interest in this study are the intralayer pair-correlation functions $g_{11}(r)$ and $g_{22}(r)$ and the mean-square displacement $\langle\Delta r^2(t)\rangle$ from which the self-diffusion coefficient D is obtained. All of these quantities can be obtained from the position vector data set alone. The relevant formulas are

$$g(r) = \frac{\langle n(r)\rangle}{2\pi r \Delta r n}, \quad (4)$$

$$\langle\Delta r^2(t)\rangle = \frac{1}{N}\left\langle \sum_{j=1}^{N} |\vec{r}_j(t)-\vec{r}_j(0)|^2 \right\rangle, \quad (5)$$

$$D = \lim_{t\to\infty}\frac{\langle\Delta r^2(t)\rangle}{4t} = \lim_{t\to\infty}\frac{1}{4}\frac{d}{dt}\langle\Delta r^2(t)\rangle, \quad (6)$$

where $\langle n(r)\rangle$ is the average number of particles in one of the layers in an annulus of radius r and thickness Δr, centered at a given particle, and N is the number of particles in the layer under consideration.

A. Pair-correlation functions

We have obtained the intralayer pair distribution functions $g_{11}(r)$ and $g_{22}(r)$ and interlayer pdf $g_{12}(r)$ for a number of values of N_2 and d. Figure 1 shows plots of $g_{11}(r)$, the lower layer pdf, for selected values of N_2 for (a) $d=0.1$ and (b) $d=0.8$. The coupling strength Γ of the lower layer is fixed at 80. The plots are staggered for clarity. From bottom to top in these graphs, $N_2=512$, 392, 288, 200, 128, 72, and 32. The x axis is r in units of a_1.

For $d=0.1$, the two layers are very close to each other and the system behaves essentially as a single layer system. The effective Γ is then about $80\sqrt{2}$ for the symmetric case which slowly decreases to 80 as N_2 decreases. Hence for all N_2, such a system is in the fluid state (solidification of a single layer electron system occurs around $\Gamma\approx 130$) and the pdfs will be representative of this state. This is exactly what is seen; however, the position R_1 of the first peak moves slowly from about 1.27 for the (512,512) symmetric bilayer to about 1.75 for the (512,32) bilayer, while the peak height is essentially constant. Since the bilayers under consideration are in

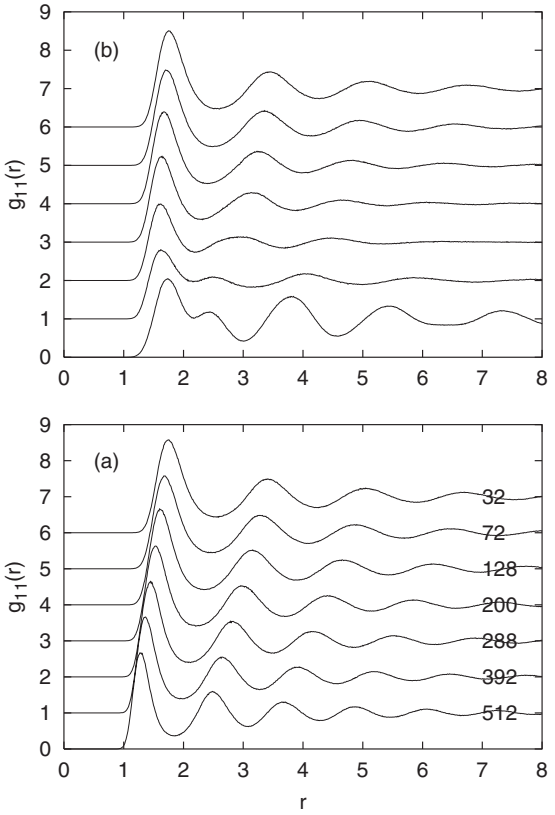

FIG. 1. Intralayer pair-correlation function $g_{11}(r)$ of the lower layer for $\Gamma_1=80$; (a) $d=0.1$ and (b) $d=0.8$; $N_2=512$, 392, 288, 200, 128, 72, and 32 (from bottom to top); d and r are in units of a_1.

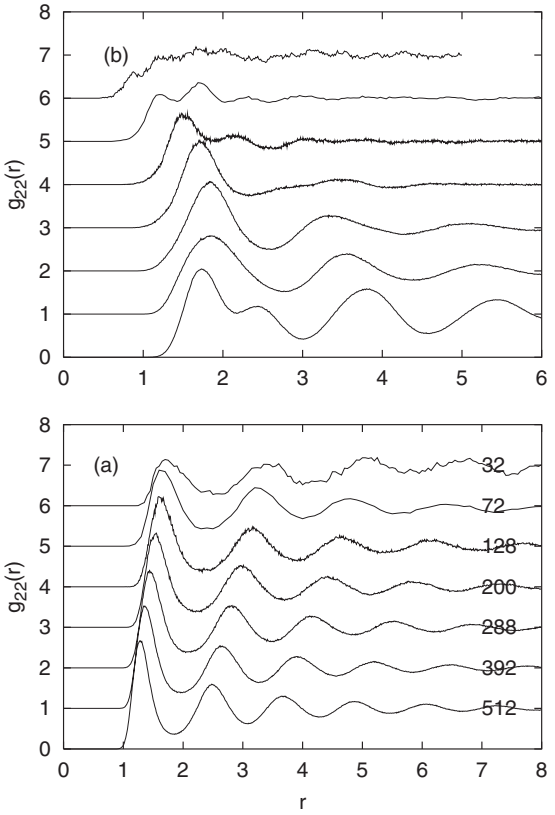

FIG. 2. Intralayer pair-correlation function $g_{22}(r)$ of the upper layer for $\Gamma_1=80$ and $N_2=512$, 392, 288, 200, 128, 72, and 32 (from bottom to top); (a) $d=0.1$ with r in units of a_1 and (b) $d=0.8$ with r in units of $a_2=\sqrt{512/N_2}$.

the strongly coupled "liquid phase," the peaks in $g_{11}(r)$ should emulate the underlying lattice structure. It has been shown[16] that a symmetric bilayer Wigner crystal possesses a simple hexagonal phase for $d\approx 0$ with a lattice constant of about 1.34 and a staggered hexagonal phase for large d with a lattice constant of about 1.88. The asymmetric (512,32) bilayer for small d would almost be equivalent to a single layer emulating a simple hexagonal phase and not a staggered one since the density of the top layer is small; however, the lattice constant would correspond to that of a symmetric bilayer at large d. This is what is reflected in the position R_1 of the first peak in $g_{11}(r)$ as we go from a symmetric bilayer to a (512,32) bilayer where the density of the upper layer is the weakest.

For $d=0.8$, where previous studies of a symmetric bilayer[1] have shown very strong interlayer correlations, the $g_{11}(r)$ plots for the asymmetric layers indicate quite a different behavior, especially for higher values of N_2. For the symmetric bilayer (lowest plot), we see the formation of a small second peak augmented by a pronounced long-range order, indicative of a solidlike behavior which has been discussed extensively.[1,2] The position of the first peak of the symmetric bilayer now reflects that of a staggered square phase with a lattice constant of about 1.76. As before, the plots then move slowly to that of a fluid phase with an underlying simple hexagonal structure for the (512,32) bilayer, and thus the peak positions do not change appreciably. For $N_2=392$, there is a remnant of the small second peak but long-range order has disappeared and it no longer mirrors a solidlike system. As N_2 is further decreased, the plots imitate that of a fluid phase and become almost identical to the $d=0.1$ plots.

Figure 2 shows plots of $g_{22}(r)$, the upper layer pdf, for various values of N_2 for (a) $d=0.1$ and (b) $d=0.8$. Here also the plots are staggered for clarity, and from bottom to top in these graphs, $N_2=512$, 392, 288, 200, 128, 72, and 32. Even though a_2 (which depends on N_2) is now a logical choice as the unit of distance, we have chosen a_1 when plotting at $d=0.1$ since the two layers are so close to each other. It also makes for easier comparison with $g_{11}(r)$. For $d=0.1$, the first peak position moves in the same way as we noted for $g_{11}(r)$. This is to be expected but we note that the peak height decreases as N_2 decreases. As N_2 decreases, a particle in the upper layer interacts with fewer particles in its own layer and with far more particles in the lower layer. This is exactly opposite in the case of a particle in the lower layer. Thus $g_{22}(r)$ is affected far more than $g_{11}(r)$ by particles in the other layer, and this becomes more pronounced as N_2 gets smaller. This seems to lower the effective Γ of the upper layer thereby reducing the peak height. For $d=0.8$, the interlayer correlations, which have been shown to manifest itself most strongly for this interlayer separation, seem to reduce the upper layer Γ considerably more in this case than for other values of d. Thus for $N_2=32$, the upper layer behaves like a dilute electron gas. It should be noted that in this plot, r is in units of a_2.

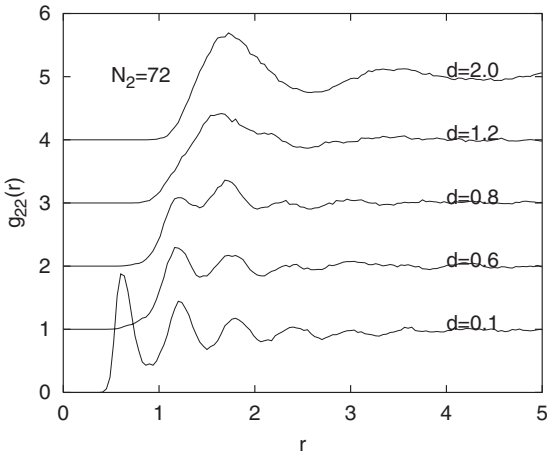

FIG. 3. Intralayer pair-correlation function $g_{22}(r)$ of the upper layer with r in units of $a_2=\sqrt{512/72}\,a_1$ for $\Gamma_1=80$, $N_2=72$, and $d=0.1$, 0.6, 0.8, 1.2, and 2.0 in units of a_1.

Figure 3 is intended to show the effect of the interlayer separations on the pdf for a significantly asymmetric system. Here are plots of $g_{22}(r)$ for various values of d for $N_2=72$. For $d=0.1$, the 512 particles in the lower layer have considerably more effect on a particle in the upper layer than do the other 71 particles in the same layer. Therefore the effective Γ of the upper layer is closer to $\Gamma_1(=80)$ than to $\Gamma_2(=30)$. Thus, we see a strong first peak and a long-range order suggestive of a strongly coupled electron liquid. For a large $d(=2.0)$, the interaction between the two layers is negligible and Γ_2 should be approximately 30, indicating a dilute electron gas. Thus the pdf has essentially one wide, soft peak with no long-range order. The intermediate values of d show the transition from one thermodynamic state to another.

Figure 4 shows plots of the interlayer pdf $g_{12}(r)$, for selected values of N_2 for (a) $d=1.2$ and (b) $d=0.8$. All the parameters are the same as for Fig. 1. For $d=0.1$, the two layers are very close to each other and the system behaves essentially as a single layer system. Thus we do not expect to see any change from the intralayer pdf $g_{11}(r)$. Even for $d=0.3$, there were no appreciable differences between $g_{11}(r)$ and $g_{12}(r)$. Thus we have plotted $g_{12}(r)$ for $d=0.8$ and 1.2. For $d=0.8$, a symmetric layer $g_{12}(r)$ does exhibit strong and long-range correlations, similar to that of $g_{11}(r)$. As N_2 is decreased, these features dissipate quickly and the height of the first peak also decreases as to be expected. For $d=1.2$, no long-range correlations exist, and as N_2 gets smaller, $g_{12}(r)$ shows just small oscillations around 1.

The effect of the interlayer separation on $g_{12}(r)$ is shown in Fig. 5 for a fixed value of $N_2=72$. The behavior is as expected; the peak heights decrease with increasing d, indicating the reduced effect of cross correlations, and for a high value of $d=2.0$, $g_{12}(r)$ is essentially flat at a value of 1.

B. Diffusion

The self-diffusion coefficients, D_1 for the lower and D_2 for the upper layer, were obtained using Eq. (6). For periodic boundary conditions, the allowed displacements of the particles are obviously bounded, but to calculate the mean-square displacements, we need the "true" atomic displacements. This is achieved by removing the effects of the wraparound through a well-established algorithm.

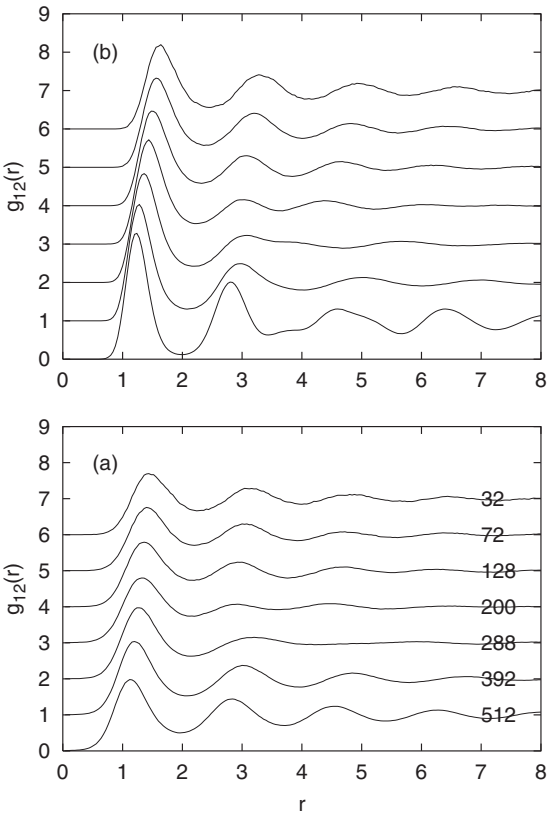

FIG. 4. Interlayer pair-correlation function $g_{12}(r)$ for $\Gamma_1=80$; (a) $d=1.2$ and (b) $d=0.8$; $N_2=512$, 392, 288, 200, 128, 72, and 32 (from bottom to top); d and r are in units of a_1.

Figure 6 shows these results (in units of a_1^2/τ) as functions of N_2 for various values of d. The solid line represents D_1, while the dashed line represents D_2. Note that the two diffusion coefficients are essentially the same for $d=0.1$. For a symmetric bilayer (512,512), the effective Γ for $d\to 0$ is $80\sqrt{2}$ with a diffusion coefficient of 0.008 which agrees with our value of D_1 (and D_2). At the other end, for (512,32), the

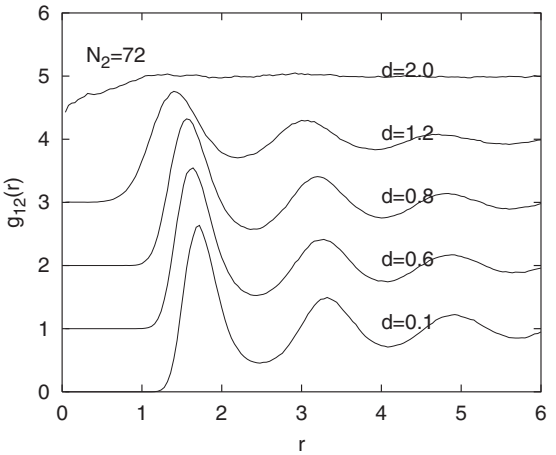

FIG. 5. Interlayer pair-correlation function $g_{12}(r)$ for $\Gamma_1=80$, $N_2=72$, and $d=0.1$, 0.6, 0.8, 1.2, and 2.0; d and r are in units of a_1.

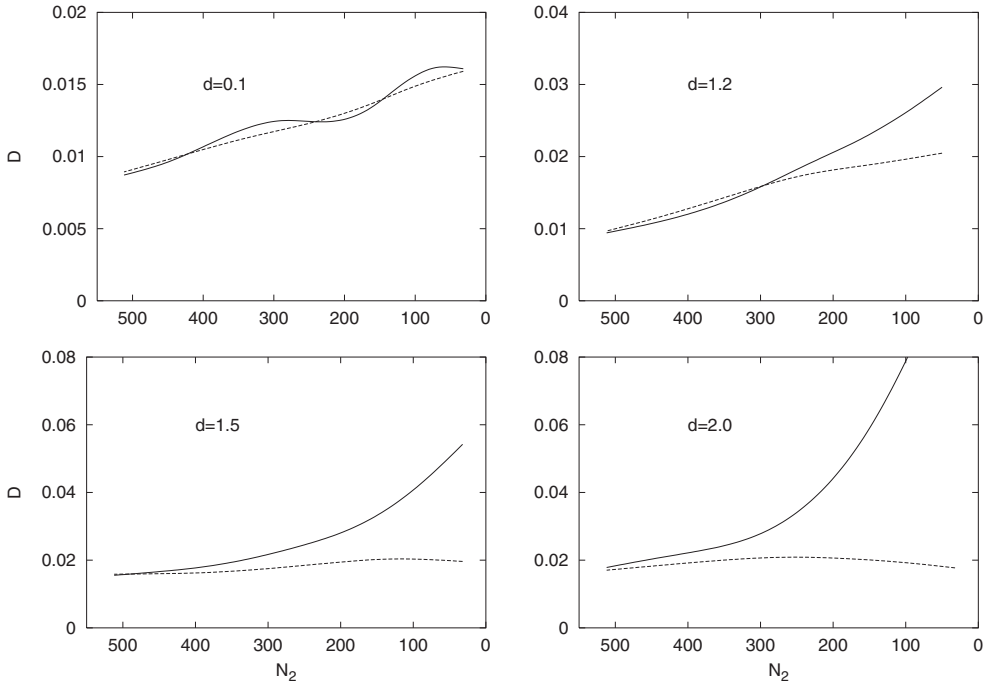

FIG. 6. Dependence of diffusion coefficients D_1 and D_2 (both in units of a_1^2/τ) on N_2 for $\Gamma_1=80$ and $d=0.1$ 1.2, 1.5, and 2.0 in units of a_1. The solid line is D_2 (upper layer), and the dashed line is D_1 (lower layer). (These curves have been smoothed.)

effective Γ for $d\to 0$ is very close to 80 with a diffusion coefficient of 0.018 which again agrees with our value of D_1 (and D_2). We do not see any deviation in the two diffusion coefficients for $d<0.8$. For $d=1.2$, the deviation sets in for $N_2<300$, while for $d=2.0$ the deviation is seen for any value of N_2. D_1 still ends up around 0.018 for $N_2=32$, for all values of d. However, the upper layer diffusion coefficient D_2 goes to much higher values. At $d=2.0$, there is negligible interaction between the two layers, and hence the respective diffusion coefficients should reflect those of an isolated layer. The plots show that this is indeed the case.

Figure 7 shows the effects of the asymmetrical density of

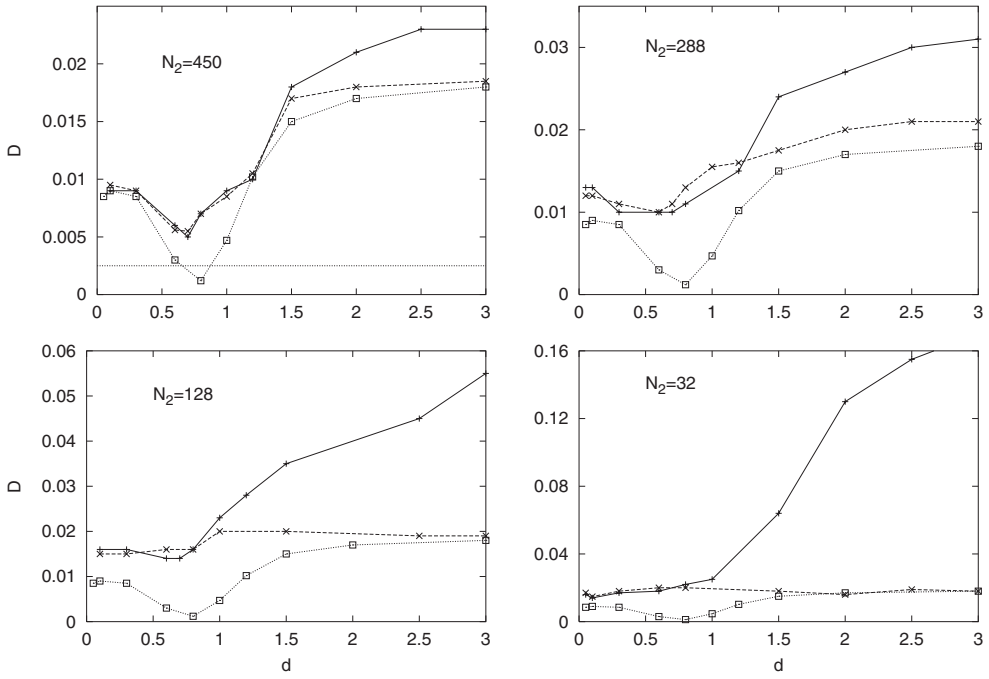

FIG. 7. Comparison of diffusion coefficients D_1 and D_2 (both in units of a_1^2/τ) as a function of interlayer separation d (in units of a_1) for $N_2=450$, 288, 128, and 32 and $\Gamma_1=80$. The solid line is D_2 (upper layer), and the dashed line is D_1 (lower layer). The diffusion coefficient for a symmetric bilayer is shown as a dotted line. The horizontal line at 0.0025 in the $N_2=450$ plot is taken to be the freezing criterion of any two-dimensional system. (Our data points are shown.)

the two layers; here are plots of the two diffusion coefficients as a function of d, for various values of N_2. The solid line is D_2 (upper layer) and the dashed line is D_1 (lower layer). The diffusion coefficient for a symmetric bilayer is shown as a dotted line. The various values of N_2 are shown inside the plots. The horizontal line at $D=0.0025$ in the plot for $N_2=450$ has been taken from a previous study[2] as the freezing criterion of any two-dimensional system. Thus we note that even the slightly asymmetric (512,450) bilayer at a coupling strength of $\Gamma_1=80$ does not exhibit a phase change for any value of d. However since the diffusion coefficients do show a dip for intermediate layer separations, a phase transition may occur in certain asymmetric layers for higher values of the coupling strength.

IV. CONCLUSIONS

We have performed extensive molecular dynamics calculations of asymmetric electron bilayers for various values of asymmetry and interlayer separations. We have analyzed, in particular, the diffusion coefficients in the two layers and the intralayer pair distribution functions. The self-diffusion coefficient of the lower layer shows only a slight dependence on the interlayer separation, whereas that of the upper layer suggests a considerable dependence. The two diffusion coefficients are basically the same for very small d but deviations set in especially for $d>1$. While a symmetric bilayer has been shown to exhibit a phase transition for some values of d, asymmetric bilayers for the chosen value of $\Gamma_1(=80)$ do not seem to have this feature even for $N_2=450$. But since the diffusion does show a dip for larger values of N_2, a higher value of Γ_1 may exhibit a phase transition.

ACKNOWLEDGMENTS

This project was supported in part by a grant from the Academic Research Program (ARP) of the Department of National Defence, Canada.

[1] Z. Donkó and G. J. Kalman, Phys. Rev. E **63**, 061504 (2001).
[2] S. Ranganathan, R. E. Johnson, and K. N. Pathak, Phys. Rev. E **65**, 051203 (2002).
[3] Z. Donkó, P. Hartmann, G. J. Kalman, and K. I. Golden, J. Phys. A **36**, 5877 (2003).
[4] S. Ranganathan and R. E. Johnson, Phys. Rev. B **69**, 085310 (2004).
[5] S. Ranganathan and R. E. Johnson, J. Phys. A **39**, 4595 (2006).
[6] L. Liu, L. Swierkowski, D. Neilson, and J. Szymanski, Phys. Rev. B **53**, 7923 (1996).
[7] G. Kalman, V. Valtchinov, and K. I. Golden, Phys. Rev. Lett. **82**, 3124 (1999).
[8] K. I. Golden and G. J. Kalman, J. Phys. A **36**, 5865 (2003).
[9] Z. Donkó and G. Kalman, J. Phys. IV **10**, Pr5-355 (2000).
[10] P. Hartmann, Z. Donkó, and G. Kalman, Europhys. Lett. **72**, 396 (2005).
[11] S. Ranganathan and R. E. Johnson, Phys. Rev. B **75**, 155314 (2007).
[12] G. J. Kalman, P. Hartmann, Z. Donkó, and K. I. Golden, Phys. Rev. Lett. **98**, 236801 (2007).
[13] H. Mahassen, K. Kutasi, K. I. Golden, G. J. Kalman, and Z. Donkó, J. Phys. A **39**, 4601 (2006).
[14] P. Ludwig, A. Filinov, Yu. E. Lozovik, H. Stolz, and M. Bonitz, Contrib. Plasma Phys. **47**, 335 (2007).
[15] R. E. Johnson and S. Ranganathan, Phys. Rev. E **63**, 056703 (2001).
[16] G. Goldoni and F. M. Peeters, Phys. Rev. B **53**, 4591 (1996).